Biomedicine & Pharmacotherapy 147 (2022) 112651

Contents lists available at ScienceDirect

Biomedicine & Pharmacotherapy

journal homepage: www.elsevier.com/locate/biopha

Decursin prevents melanogenesis by suppressing MITF expression through the regulation of PKA/CREB, MAPKs, and PI3K/Akt/GSK-3β cascades

Hyungyeong Choi [a], Jeong-Hyun Yoon [a], Kumju Youn [b], Mira Jun [a,b,c,*]

[a] Department of Health Sciences, The Graduate School of Dong-A University, Busan 49315, South Korea
[b] Department of Food Science and Nutrition, Dong-A University, Busan 49315, South Korea
[c] Institute of Convergence Bio-Health, Dong-A University, Busan 49315, South Korea

ARTICLE INFO

Keywords:
Anti-melanogenesis
Decursin
MAPK
MITF
PKA/CREB
PI3K/Akt/GSK-3β

ABSTRACT

Abnormal melanin synthesis upon UV exposure causes excessive oxidative stress, which leads to skin hyperpigmentation disorders such as freckles, melisma, and age spots. The present study investigated the anti-melanogenic effects of decursin and the underlying mechanism using multiple approaches. Decursin exhibited no cytotoxicity and significantly reduced intracellular tyrosinase activity and melanin content in B16F10 melanoma cells. Decursin also inhibited the expression of melanogenic enzymes such as tyrosinase and tyrosinase-related protein (TRP)− 1, but not TRP-2. Mechanistically, decursin suppressed melanin synthesis through cAMP-dependent protein kinase (PKA)/cAMP response element-binding protein (CREB)-dependent downregulation of microphthalmia-associated transcription factor (MITF), a master transcription factor in melanogenesis. Further, decursin exerted anti-melanogenic effects by downregulating the p38 signaling pathway and upregulating extracellular signal-regulated kinase (ERK) and phosphatidylinositol 3 kinase (PI3K)/protein kinase B (Akt)/glycogen synthesis kinase-3β (GSK-3β) cascades. *in silico* analysis showed that decursin formed specific interactions with residues of upstream regulators of MITF and exhibited optimal pharmacokinetic profiles, including permeability and skin sensitization. Finally, the anti-melanogenic effects of decursin were confirmed *ex vivo* in 3D human skin models, suggesting its applicability as a protective agent against hyperpigmentation.

1. Introduction

Melanin is responsible for the color of the skin, eye, and hair, and performs important protective functions against ultraviolet (UV) irradiation. Melanin synthesized in melanosomes within melanocytes is transferred to the surrounding keratinocytes where it plays an essential role in photoprotection [1]. However, chronic UV exposure stimulates abnormal production of melanin, leading to hyperpigmentation disorders such as freckles, melasma, and age spots. Melanocytes produce two types of melanin, namely, pheomelanin (red/yellow pigment) and eumelanin (brown/black pigment). Melanogenesis is mainly regulated by tyrosinase, a rate-limiting enzyme, which promotes the conversion of tyrosine to dihydroxyphenylalanine (DOPA) as well as the further oxidation of DOPA to DOPA quinone. This step is common in both eumelanin and pheomelanin production. The subsequent steps involve two additional enzymes, tyrosinase-related protein 1 (TRP-1) and TRP-2, to produce eumelanin [2].

Microphthalmia-associated transcription factor (MITF) is widely expressed in various cell types, including retinal pigment epithelium, mast cells, osteoclasts, heart cells, and melanocytes [3]. There are at least 10 different isoforms of MITF distinguished by unique amino-terminal structures that exhibit tissue-specific expression patterns. Among these, the M isoform of MITF selectively expressed in the melanocyte cell lineage is a master regulator that plays an essential role in the development, differentiation, and survival of melanocytes [4]. Furthermore, the regulator transcriptionally controls crucial melanogenesis-related enzymes, including tyrosinase, TRP-1, and TRP-2 [5]. Recent studies have shown that MITF mutations are related to different clinical presentations of Waardenburg syndrome, including hypopigmentation and deafness, owing to melanocyte deficiency in

Abbreviations: TRP, tyrosinase-related protein; PKA, cAMP-dependent protein kinase; CREB, cAMP response element-binding protein; MITF, microphthalmia-associated transcription factor; ERK, extracellular signal-regulated kinase; PI3K, phosphatidylinositol 3 kinase; Akt, protein kinase B; GSK-3β, glycogen synthesis kinase-3β; α-MSH, α-melanocyte-stimulating hormone; MAPK, mitogen-activated protein kinase; JNK, c-Junction N-terminal kinase.

* Corresponding author at: Department of Health Sciences, The Graduate School of Dong-A University, Busan 49315, South Korea.
E-mail addresses: hyungyung2@donga.ac.kr (H. Choi), yjhyun1110@donga.ac.kr (J.-H. Yoon), kjyoun@dau.ac.kr (K. Youn), mjun@dau.ac.kr (M. Jun).

https://doi.org/10.1016/j.biopha.2022.112651
Received 18 November 2021; Received in revised form 7 January 2022; Accepted 13 January 2022
Available online 18 January 2022

humans [6,7].

The signaling pathway for MITF-induced melanogenesis has been found to primarily involve the cAMP-dependent protein kinase (PKA)/cAMP response element-binding protein (CREB) axis [8]. Upon exposure to UV, α-melanocyte-stimulating hormone (α-MSH) binds to melanocortin 1 receptor and elevates the intracellular levels of cAMP, leading to the activation of PKA. PKA then translocates to the nucleus and subsequently phosphorylates CREB [9]. Activated CREB directly binds to the *MITF* gene promoter and induces expression of MITF, which in turn stimulates the transcription of downstream target melanogenic genes.

Mitogen-activated protein kinases (MAPKs) are evolutionarily conserved enzymes connecting cell surface receptors to critical regulatory targets within cells [10]. The association of MITF with the MAPK pathway was first highlighted by the discovery that it is phosphorylated by extracellular signal-regulated kinase (ERK) for ubiquitin-mediated proteasomal degradation [11]. In contrast, it has been shown that phosphorylation of stress-regulated protein kinase (p38) and c-Junction N-terminal kinase (JNK) trigger melanogenesis by stabilizing MITF activation [12].

Glycogen synthase kinase-3β (GSK-3β), a ubiquitously expressed and evolutionarily conserved kinase, has been identified as an enzyme that regulates glycogen synthesis and expression of tau, a neuronal microtubule-associated protein [13,14]. GSK-3β directly regulates the transcriptional level of MITF and the consequent MITF-mediated melanin synthesis [15]. It has been recently demonstrated that the activation of the phosphatidylinositol 3 kinase (PI3K)/protein kinase B (also known as Akt) axis results in the phosphorylation of GSK-3β at Ser 9, and eventually leads to the downregulation of MITF expression [16].

Angelica gigas Nakai (*A. gigas* Nakai), known as Korean Angelica, has been used as a traditional herbal medicine or food in Asian countries, including China, Japan, and Korea [17]. It has several pharmacological properties, including antinociceptive, antitumor, anti-amnestic, and neuroprotective activities [18–21]. In addition, Lv et al. (2007) demonstrated the hypopigmenting effect of an extract of *A. gigas* Nakai against isobutylmethylxanthine (IBMX)-induced melanogenesis in B16 melanoma cells [22]. Pyranocoumarins, including decursin, decursinol, and decursinol angelate, are the major components identified in *A. gigas* Nakai [23]. In our effort to discover natural candidates with potent and safe anti-melanogenic effects, we focused on the major compounds of *A. gigas* Nakai. Our preliminary study revealed decursin as the most potent component of the extract. In the present study, we designed a novel approach to elucidate the anti-melanogenic properties of decursin through regulation of the PKA/CREB, MAPK, and PI3K/Akt/GSK-3β signaling pathways in B16F10 cells and an *ex vivo* human skin model. Furthermore, we evaluated the molecular binding conformation with targeted proteins and pharmacokinetic properties of decursin using an *in silico* docking and pharmacokinetic simulation.

2. Materials and methods

2.1. Chemicals and reagents

Decursin (≥97%), 3-(4,5-dimethyl-thiazol-2-yl)− 2, 5-diphenyl tetrazolium bromide (MTT), L-DOPA, H89, SB203580, PD98059, LY294002, and dimethylsulfoxide (DMSO) were bought from Sigma-Aldrich (St. Louis, MO, USA). Dulbecco's modified Eagle's medium (DMEM) and phosphate-buffered saline (PBS) were from Welgene (Daegu, Korea). Fetal bovine serum (FBS) and penicillin/strepcomycin were purchased from Hyclone Laboratories (Logan, UT, USA).

The primary antibodies for TYR, TRP-1, TRP-2, MITF, GSK-3β, JNK, ERK 1/2 and β-actin were obtained from Santa Cruz Biotechnology Inc. (Santa Cruz, CA, USA). CREB was bought from Gene Tex Inc. (San Diego, CA, USA). p-GSK-3β, p-JNK, p-ERK 1/2, p-p38, p38, Akt, p-Akt, CREB, and p-CREB were purchased from Cell Signaling Technology Inc. (Beverly, MA, USA). The secondary antibodies (anti-mouse IgG and anti-rabbit IgG) conjugated with horseradish peroxidase were from Santa Cruz Biotechnology Inc.

2.2. Cell culture and sample treatment

B16F10 melanom-a cells were obtained from the Korean Cell Line Bank (Seoul, Korea). Cells were cultured in DMEM supplemented with FBS and penicillin/streptomycin in a humidified incubator of 5% CO_2 at 37 °C. Young B16F10 cells (less than 20 passages) were used that significantly overproduced intracellular melanin contents compared with older cells (over 20 passages). Decursin was solubilized in DMSO and diluted to various concentrations. Control groups were treated with equal concentrations of DMSO (≤ 0.1%).

2.3. Cell viability

B16F10 cells (3×10^3 cells/well) were seeded in each well of 96-well and cultured in an incubator for 24 h. The medium was then was replaced with DMEM containing decursin at 10, 20, 30 and 40 μM concentrations. After incubation for 72 h, MTT reagent (5 mg/mL) was added to the cells for 3 h at 37°C. The cells were lysed in DMSO and the absorbance at 570 nm was measured by a microplate reader (ELX808, BioTek, Winooski, VT, USA). The percentage of cell viability was measured by comparing 100% viability of untreated cells (control groups).

2.4. Determination of melanin content

B16F10 melanoma cells (2.0×10^5 cells/well) were seeded into the 6-well culture plates. After 24 h of incubation, the cells were treated with/without various concentration of sample in DMEM. Following the treatment for 72 h., the cells were washed twice and collected using PBS. The collected cells were centrifuged and then dissolved in 1 N NaOH at 95 °C for 1 h. The aliquots of cell lysates were transferred to 96-well culture plates and the absorbance of melanin contents were estimated by ELISA microplate reader at 405 nm. The melanin contents were calculated as percentages of change to untreated cells [24].

2.5. Measurement of cellular tyrosinase activity

Tyrosinase activity was evaluated using L-DOPA as a substrate. B16F10 cells were plated in 6-well culture plate for overnight and then treated with/without indicated concentration of decursin or kojic acid. After 72 h, the cells were harvested with PBS and lysed in a 1 × cell lysis buffer for 1 h on ice and centrifuged for 20 min at 13,000 rpm. The protein quantification of the supernatant was then using a BCA assay kit. Potassium phosphate buffer (100 mM, pH 6.8), cell lysates (50 μg) and 10 mM L-DOPA solution were placed in a 96-well culture plates at 37 °C for 1 h. The mixtures were measured by a microplate reader at 490 nm [25].

2.6. Western blot analysis

Once the B16F10 cells were collected, the cell pellets were lysed in a 1 × cell lysis buffer for 1 h on ice. The protein concentration of cell lysates was equally adjusted at 20 μg and denatured with a protein 5 × sample buffer (Elpis Biotech, Daejeon, Korea) for 5 min at 95 ℃. The samples were separated from SDS-polyacrylamide gel electrophoresis and transferred to PVDF membranes. The membranes were blocked using a 5% skim milk (BD Biosciences, San Jose, CA, USA) for 3 h at room temperature, and then washed in Tris-Buffered Saline with Tween 20 (TBST) buffer, followed by incubated overnight with primary antibodies against TYR (1:500), TRP-1 (1:2000), TRP-2 (1:500), MITF (1:500), Akt (1:1000), p-Akt (1:1000), GSK-3β (1:1000), JNK (1:1000), ERK 1/2 (1:1000), CREB (1:1000), p-GSK-3β (1:1000), p-JNK (1:1000), p-ERK 1/2 (1:1000), p-p38 (1:1000), p38 (1:1000), p-CREB (1:2000) and β-actin (1:10000). After rinsing with TBST buffer, the membranes

were incubated at room temperature for 10 min with secondary antibodies, anti-rabbit (1:7000) or anti-mouse IgG (1:7000). Protein bands detections were using the ECL reagents (Advansta Inc, Menlo Park, CA, USA) and visualized by Atto EZ-capture imaging system (Tokyo, Japan). The band images were analyzed using the ImageJ software (NIH, Bethesda, MD, USA).

2.7. ex Vivo 3D human skin model

3D human epidermis skin models (Neoderm®-ME) containing human-derived melanocytes were purchased from Tego Science (Seoul, Korea). The 3D human epidermis models were transferred to a 12-well culture plate with maintenance medium (Tego Science) and cultured in an incubator of 5% CO_2 at 37 °C for 1 day. Decursin stock or DMSO (control groups) was diluted with PBS to indicated concentrations and applied once every three days to the surface of the 3D human skin models and the maintenance medium was changed together when decursin was applied. After 15 days, Fontana-Masson staining was performed for the melanin contents quantification.

2.8. Fontana-Masson staining assay

Skin tissues were fixed with 4% formaldehyde and embedded in paraffin blocks. Paraffin sectioned skin tissue slides were melted in a 60 °C dry oven for 1 h. Each slide was immersed in xylene 3 times for 15 min, followed by dehydrated twice in 95% EtOH and 2 times in 100% EtOH. Then, the slides were washed using distilled water. FM staining of tissues were performed according to the manufacturer's protocol (ab150669, Abcam, Waltham, MA, USA). The sections were added to an ammoniacal silver solution and incubated at 58 °C for 30 min, then rinsed several times with distilled water. It was then incubated in 0.2% gold chloride solution for 30 s. After rinsing again with distilled water, 5% of sodium thiosulfate solution was placed at room temperature for 1–2 min. After that, sections were washed with running tap water for 2 min and 2 changes of distilled water. And then, incubate slide in nuclear fast red solution for 5 min, rinsed with running tap water, and distilled water was exchanged twice. Finally, it was dehydrated very quickly three times in fresh absolute alcohol. Subsequently, the skin tissue sections were observed by magnifying 400 × using a microscopy (Olympus, Tokyo, Japan) and the melanin content was quantified using the ImageJ program [26].

2.9. in Silico docking analysis and pharmacokinetic prediction

The simplified molecular input line entry system (SMILES) format of decursin by ChemSketch software was entered into the pkCSM to assess pharmacokinetic profiles [27].

The 3D structure of decrusin (CID: 442126) was cited from PubChem. Crystallographic structure of PKA (PDB: 1CX4), p38 (PDB: 3ZS5), ERK (PDB: 5KE0), and PI3K (PDB: 4JPS) was obtained from Protein Data Bank. Docking simulation was conducted using AutoDock Vina 1.1.2 [28]. Binding geometries and interactions were visualized by PyMOL 2.5.0 version. The pharmacophore of hydrogen bonds and Van der Waals interactions was performed with Ligplot^{+} program.

2.10. Statistical analysis

All results were expressed as the mean ± SD and repeated at least three times. Using a statistical analysis system (SAS), statistical differences between multiple groups were performed by Duncan's test and comparison between the two groups was performed by student t-test. The statistical significance of the p-value was considered *$p < 0.05$, * *$p < 0.01$, * **$p < 0.001$.

3. Results

3.1. Decursin reduced melanin production and tyrosinase activity in B16F10 cells

The chemical structure of decursin is shown in Fig. 1 A. We evaluated the cytotoxicity of decursin against B16F10 melanoma cells, and found that decursin did not exert any toxicity up to 30 μM concentration. However, it significant affected cell viability at 40 μM concentration (Fig. 1B). Therefore, we conducted further experiments at concentrations lower than 40 μM. As shown in Fig. 1 C, decursin remarkably reduced the melanin content as compared with 500 μM kojic acid, a positive control known to exhibit strong whitening effects. Consistently, the tyrosinase activity also dose-dependently decreased in cells pretreated with decursin (Fig. 1D). In particular, the compound at 30 μM concentration decreased intracellular tyrosinase activity by 59.8 ± 0.6% as compared with the control treatment. Kojic acid exhibited only 77.5 ± 3.7% inhibition even at 500 μM concentration.

3.2. Decursin regulated the expression of melanogenesis-related proteins

Decursin significantly downregulated the protein levels of tyrosinase and TRP-1 at all tested concentrations but had no effect on TRP-2 expression (Fig. 1E-H). In particular, tyrosinase expression was suppressed by approximately 50% by decursin even at the lowest tested concentration. The protein expression of MITF, a major upstream transcription factor of TRPs, was reduced by decursin in a dose-dependent manner (Fig. 1E and I). These results clearly suggest that decursin inhibited melanogenesis via MITF-mediated downregulation of tyrosinase and TRP-1, but not TRP-2.

3.3. Decursin inhibited melanogenesis through the PKA/CREB signaling pathway

The inhibitory effects of decursin on MITF-induced expression of tyrosinase and TRP-1 and melanin production suggest its possible suppressive effects on the expression of CREB, an upstream transcription regulator of MITF. Indeed, decursin treatment significantly downregulated the expression level of phosphorylated CREB as compared with the control treatment (Fig. 2A).

PKA activation enhances CREB and target gene expression. The involvement of PKA in the downregulation of CREB phosphorylation by decursin was confirmed using H89, a selective and potent inhibitor of PKA. Pre-treatment with H89 at 10 μM concentration significantly attenuated melanin production and tyrosinase activity by 47.6 ± 0.6% and 50.3 ± 8.8%, respectively, as compared with the untreated control (Fig. 2B and C). Melanin content and tyrosinase activity were lower in cells co-treated with decursin and H89 than in those treated with decursin alone ($p < 0.001$). Moreover, the expression of tyrosinase, TRP-1, and MITF obviously decreased after co-treatment with decursin and H89 (Fig. 2D-G). Decursin-mediated downregulation of CREB phosphorylation at 30 μM concentration was markedly attenuated upon co-treatment with 10 μM H89 (Fig. 2H). Thus, the anti-melanogenesis effect of decursin closely involves the PKA/CREB signaling pathway.

3.4. Decursin suppressed melanogenesis via the p38 and ERK/MAPK signaling pathway

We evaluated the phosphorylation of p38, ERK, and JNK MAPKs to investigate the upstream cascade related to the anti-melanogenesis effect of decursin. As shown in Fig. 3A-C, decursin treatment remarkably reduced the levels of phosphorylated p38 and significantly augmented ERK phosphorylation as compared to control treatment. However, the compound exerted no significant effect on JNK phosphorylation (Fig. 3A and D). Thus, both p38 suppression and ERK activation by decursin were partly associated with anti-melanogenesis.

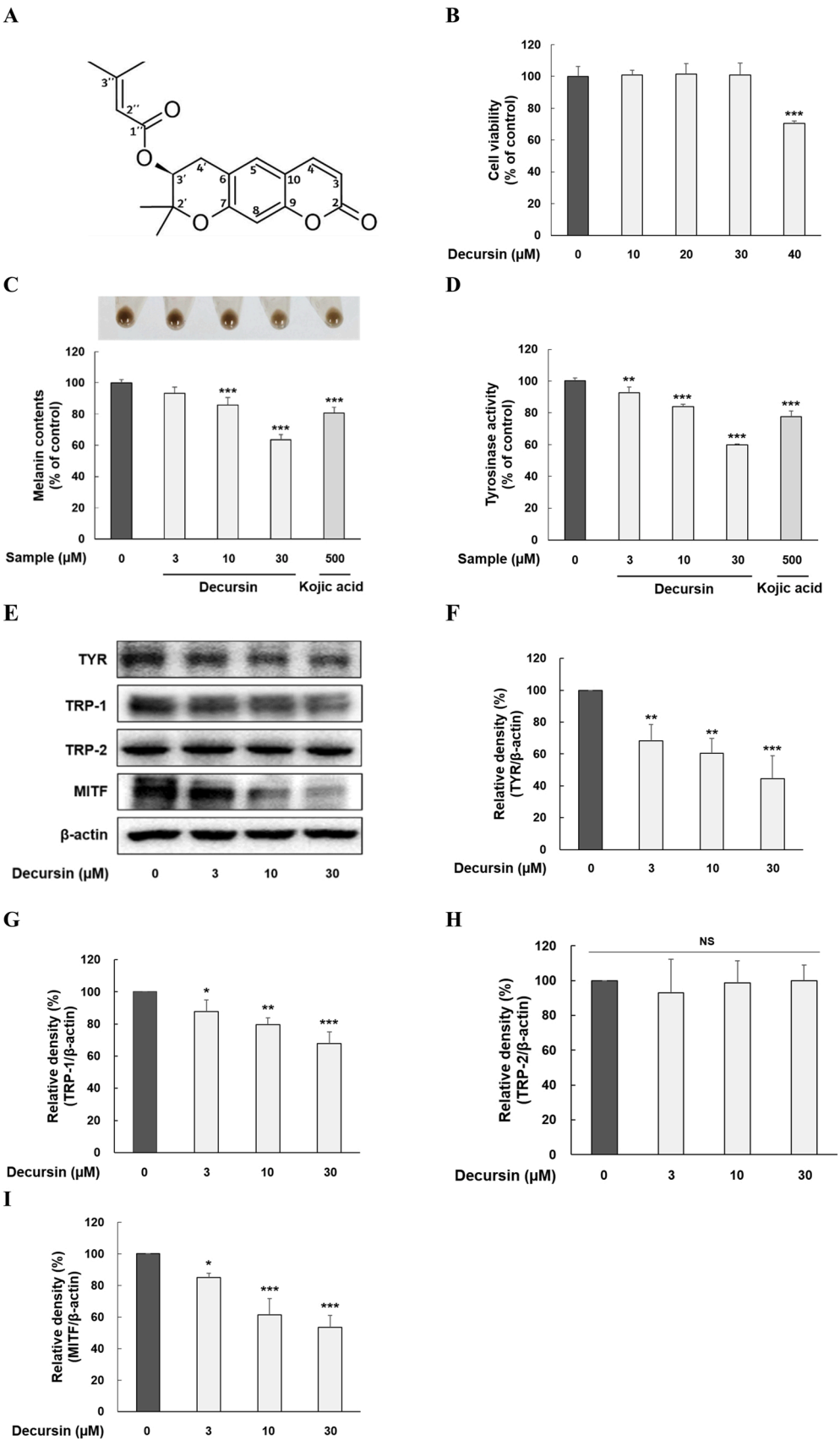

Fig. 1. Effect of decursin on the viability, melanin production, tyrosinase activity, and melanogenesis-related protein expression of B16F10 cells. (A) Chemical structure of decursin. (B) Cell viability was evaluated by the MTT assay. Cultured B16F10 cells were pre-treated with decursin (3, 10, 30 μM) for 72 h. (C) Cells were collected and centrifuged to obtain pellets. The pellets were dissolved in 1 N NaOH, and the relative amount of melanin was determined by measuring the absorbance at 405 nm. (D) After treatment under the same conditions used for the determination of melanin synthesis, cells were collected and lysed. Tyrosinase activity was measured using L-DOPA as a substrate. Cell viability, melanin contents, and tyrosinase activity in control cells were regarded as 100%. (E-I) Cells were treated with decursin at indicated concentrations for 48 h and then harvested. Protein extracts were prepared from each treatment group, and the expression of tyrosinase (TYR), TRP-1, TRP-2, and MITF was determined by western blotting. The relative intensity of the protein band was quantified using ImageJ software, and the value was normalized to that of the corresponding loading control. Untreated cells were regarded as 100%. Values are shown as the mean ± SD of least three independent experiments. * **$p < 0.001$, * *$p < 0.01$ and *$p < 0.05$ as compared with the control group. NS; not significant.

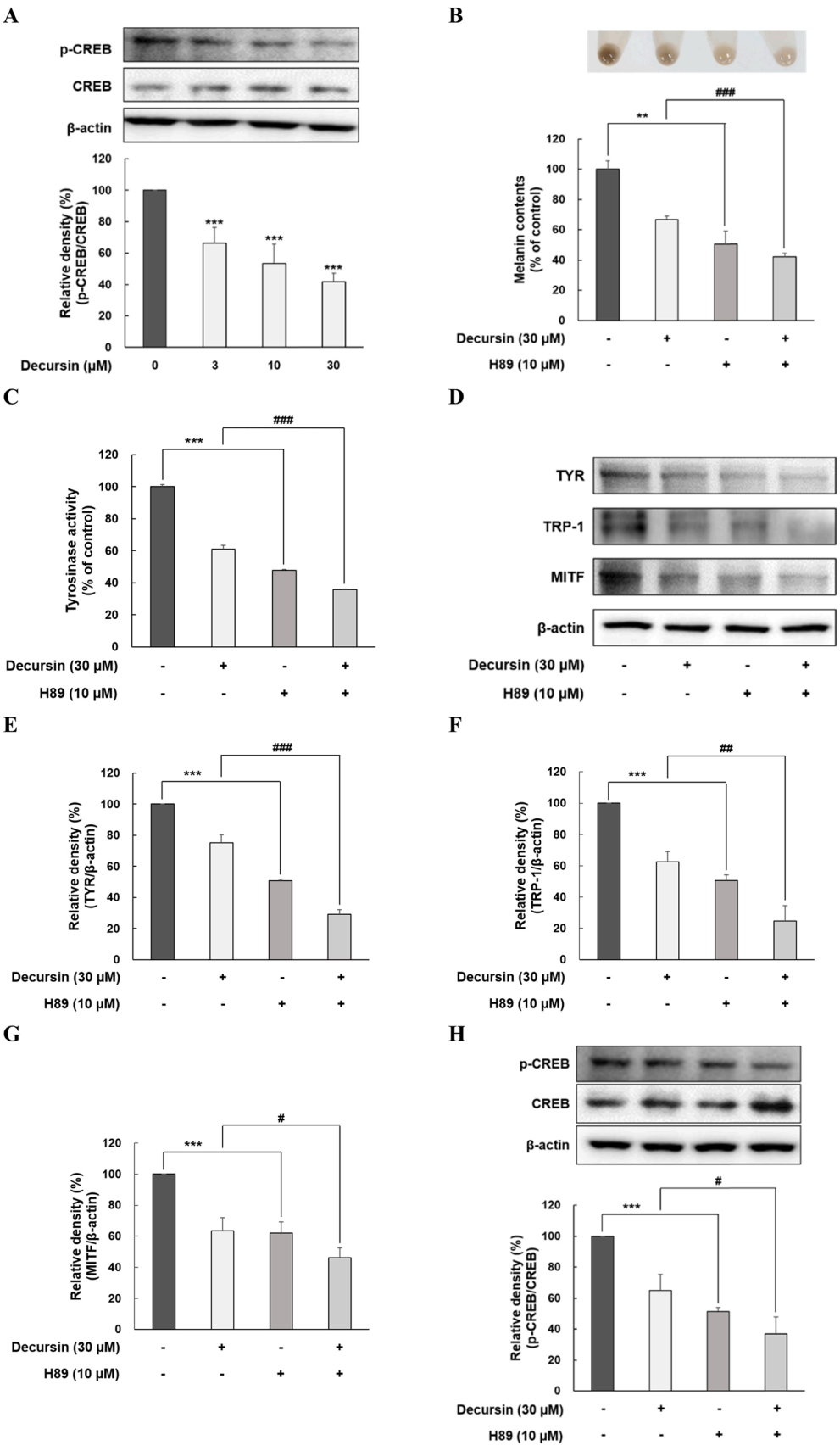

Fig. 2. Inhibitory effect of decursin on PKA/CREB-stimulated melanin accumulation and melanogenesis-related protein expression. Cells were treated with decursin at indicated concentrations for 24 h and then harvested. (A) Protein extracts were prepared from each treatment group, and the expression of p-CREB was determined by western blotting. (B, C) B16F10 cells were co-treated with H89 (PKA inhibitor, 10 μM) and decursin (30 μM) for 72 h to evaluate cellular melanin contents and tyrosinase activity. (D-G) Cells were treated with H89 (10 μM) for 30 min and then incubated with decursin (30 μM) for 48 h. The expression of tyrosinase (TYR), TRP-1, and MITF was determined by western blotting. (H) Western blotting result of p-CREB expression following co-treatment with H89 and decursin. The relative intensity of the protein band was quantified using ImageJ software, and the value was normalized to that of the corresponding loading control. Untreated cells were regarded as 100%. Values are shown as the mean ± SD of least three independent experiments. * **$p < 0.001$, * *$p < 0.01$ and *$p < 0.05$ as compared with the control group; ###$p < 0.001$, ##$p < 0.01$ and #$p < 0.05$ as compared with decursin group without H89.

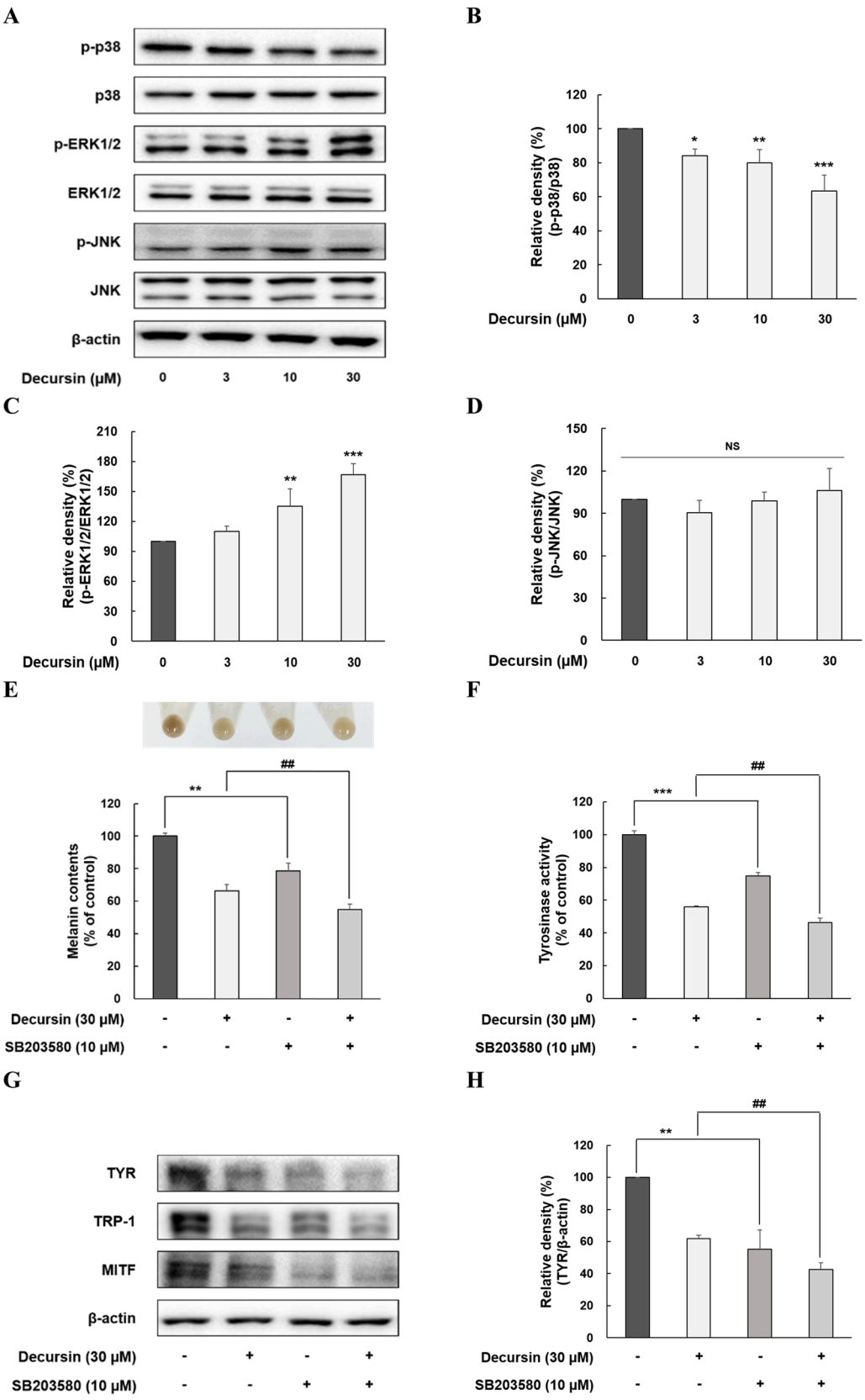

Fig. 3. Effect of decursin on MAPK-dependent melanogenesis. (A-D) Cells were treated with decursin at indicated concentrations for 1 h and then harvested. Protein extracts were prepared from each treatment group, and the expression of p-p38, p-ERK, and p-JNK was determined by western blotting. (E, F) B16F10 cells were co-treated with SB203580 (p38 inhibitor, 10 μM) and decursin (30 μM) for 72 h to evaluate cellular melanin contents and tyrosinase activity. B16F10 cells were treated with SB203580 (10 μM) for 30 min, followed by treatment with decursin (30 μM). The expression of (G-J) tyrosinase (TYR), TRP-1, MITF, and (K) p-p38 was determined by western blotting. (L, M) B16F10 cells were co-treated with PD98059 (ERK inhibitor, 10 μM) and decursin (30 μM) for 72 h to evaluate cellular melanin contents and tyrosinase activity. The expression of (N-Q) TYR, TRP-1, MITF, and (R) p-ERK was determined by western blotting. The relative intensity of the protein band was quantified using ImageJ software, and the value was normalized to that of the corresponding loading control. Un treated cells were regarded as 100%. Values are shown as the mean ± SD of least three independent experiments. $^{***}p < 0.001$, $^{**}p < 0.01$ and $^{*}p < 0.05$ as compared with the control group; $^{\#\#\#}p < 0.001$, $^{\#\#}p < 0.01$ and $^{\#}p < 0.05$ as compared with decursin group without SB203580 or PD98059. NS; not significant.

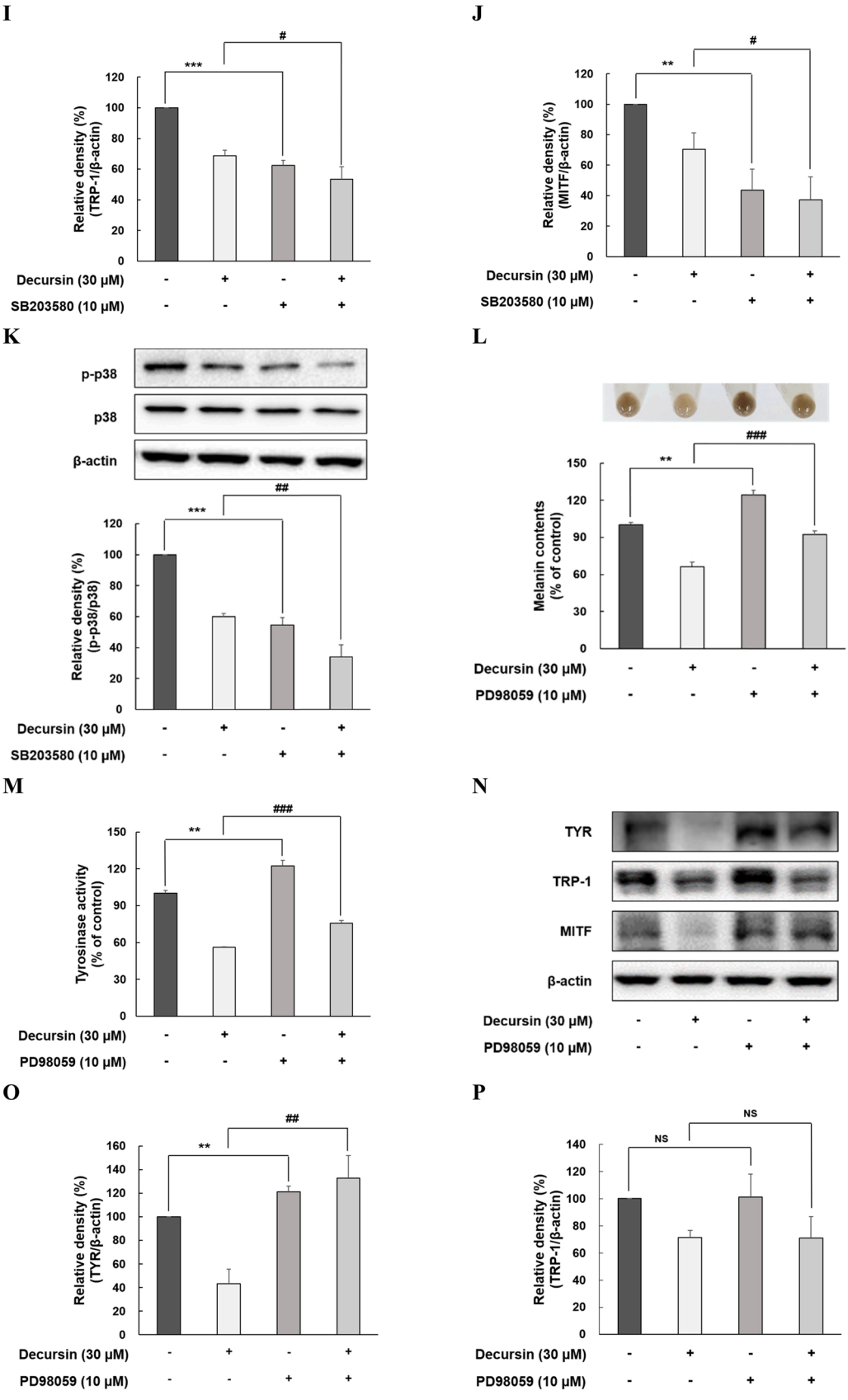

Fig. 3. (*continued*).

We also investigated the effects of decursin in both the presence and absence of MAPK-selective inhibitors, including p38 (SB203580) and ERK (PD98059), to understand the signaling cascades underlying this anti-melanogenesis property. As shown in Fig. 3E and F, co-treatment with decursin and SB203580 led to more effective inhibition of melanin expression and tyrosinase activity than decursin treatment

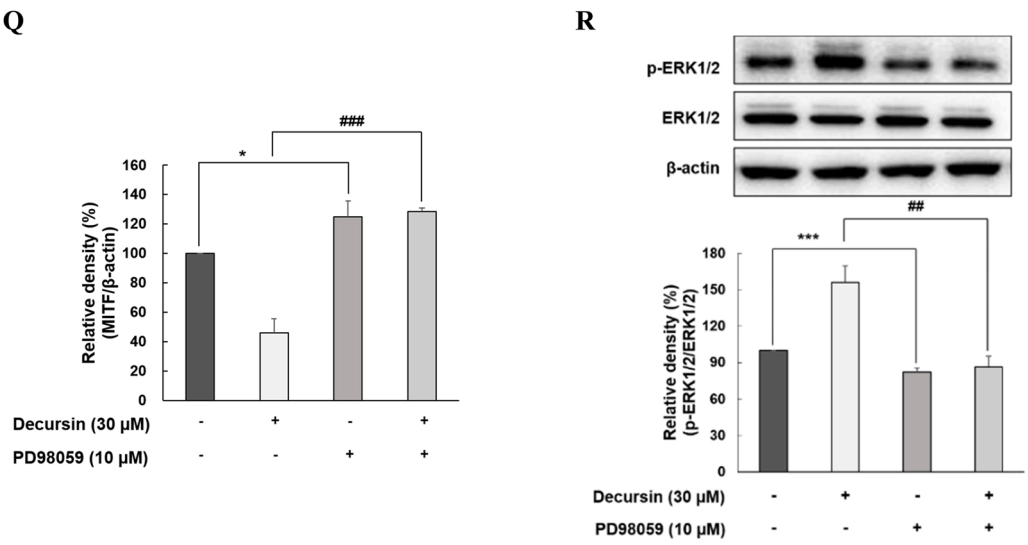

Fig. 3. (*continued*).

alone. In addition, the combination of decursin and SB203580 significantly inhibited p38 expression as well as the expression of MITF and its downstream target proteins such as tyrosinase and TRP-1 as compared with decursin alone. Therefore, the anti-melanogenic activity of decursin is dependent on the p38 cascade (Fig. 3G-K). We blocked the ERK signaling pathway by co-treating cells with a specific ERK inhibitor, PD98059, and decursin and found that both the melanin content and tyrosinase activity were considerably higher in the co-treatment group than in the cells treated with decursin alone (Fig. 3 L and M). In addition, tyrosinase and MITF gene expression, but not TRP-1 expression, was elevated after co-treatment with decursin and PD98059 (Fig. 3N-Q). As depicted in Fig. 3R, the combination of decursin and PD98059 noticeably downregulated ERK activation induced by decursin.

3.5. Decursin repressed melanogenesis through PI3K/Akt/GSK-3β signaling pathways

GSK-3β phosphorylation by PI3K/Akt has been shown to induce MITF degradation and inhibit melanogenesis [13]. As illustrated in Fig. 4A-C, the phosphorylation of GSK-3β and Akt remarkably increased in decursin-treated cells as compared to that in the control group.

To further confirm the contribution of the PI3K/Akt/GSK-3β signaling pathway in decursin-mediated inhibition of MITF-induced hyperpigmentation, we treated cells with a PI3K-specific inhibitor (LY294002). The inhibition of melanin content and tyrosinase activity after decursin treatment was diminished upon co-treatment with decursin and LY294002 ($p < 0.001$, Fig. 4D and E). Similarly, the combination of decursin and LY294002 reversed the effect of decursin on the protein levels of tyrosinase, TRP-1, and MITF (Fig. 4F-I). Finally, co-treatment with decursin and LY294002 suppressed the decursin-induced upregulation in Akt and GSK-3β phosphorylation, suggesting that PI3K/Akt/GSK-3β is an important signaling pathway involved in mediating the inhibitory effect of decursin on melanogenesis (Fig. 4J-L).

3.6. Decursin suppressed melanin synthesis in a 3D human skin model

The 3D skin model was proven to exhibit morphological equivalence with the human skin and represented an in vivo-like histological morphology characterized with a multi-layered, stratified, and pigmented epidermis [29–32]. We used this pigmented 3D human skin model to confirm our results observed in the B16F10 cell culture system. Images of Fontana-Masson-stained tissue sections indicated that melanin accumulation in the epidermis substantially decreased after treatment with decursin at all concentrations (Fig. 5). Interestingly, decursin at 10 and 30 μM doses reduced melanin content by 48.9 ± 8.7% and 33.8 ± 9.1%, respectively.

3.7. Molecular docking of decursin

To understand the mechanism underlying the interaction between decursin and the upstream regulator of MITF, a docking simulation was conducted. The docking results (Fig. 6A and Table 1) revealed the binding to PKA with the lowest energy of − 7.8 kcal/mol. In addition, the compound formed a hydrogen bond with Gln377 and van der Waals interactions with Asp149, Asn212, Asp214, Arg216, Gly217, Ala308, Asp309, Asp375, and Val376. The decursin-PKA complex was stabilized by the formation of a hydrogen bond between Gln377 residue and the oxygen group of decursin with a bonding distances of 3.3 Å.

The binding of decursin to the active site of p38 is shown in Fig. 6B and Table 1. The Decursin-p38 complex had the lowest binding energy (−8.0 kcal/mol). The complex was stabilized by the formation of a hydrogen bond between His64 residue and the oxygen group at C-2 of decursin with a bonding distance of 3.01 Å. In addition, 10 van der Waals interactions were observed with Tyr35, Lys53, Leu55, Ser56, Arg57, Pro58, Arg67, Thr68, Glu71, Asp168, and Phe169. Tyr35 and Lys53 are part of the p38 active site.

As illustrated in Fig. 6C and Table 1, a hydrogen bond was observed between decursin and ERK residues, with the lowest binding energy of − 8.1 kcal/mol. The Ser206 residue of ERK participated in the formation of a hydrogen bond with the oxygen group at C-7 of decursin with a bonding distance of 2.88 Å. The binding site for the decursin-ERK complex was formed by van der Waals interactions with Pro174, Asp177, Asn199, Thr204, Lys205, Ile254, Pro296, and His297.

Decursin was best docked to PI3K with a binding energy of − 9.0 kcal/mol. It interacted with PI3K through van der Waals interactions with Pro3, Arg4, Glu76, Arg93, Phe119, Gly122, Lys672, Met675, His676, Val706, and Glu710 (Fig. 6D and Table 1).

3.8. Pharmacokinetic profiles of decursin for bioavailability

The information on pharmacokinetic and toxicological properties is important to understand the in vivo efficacy and safety of the target compound. The design of novel agents requires substantial attention to their pharmacokinetic properties, including intestinal absorption, penetration and sensitization of skin, and mutagenic response (AMES).

As shown in Table 2, decursin was predicted to penetrate the stratum corneum, which is mostly responsible for the skin barrier function. In addition, the compound showed human intestinal absorption across the

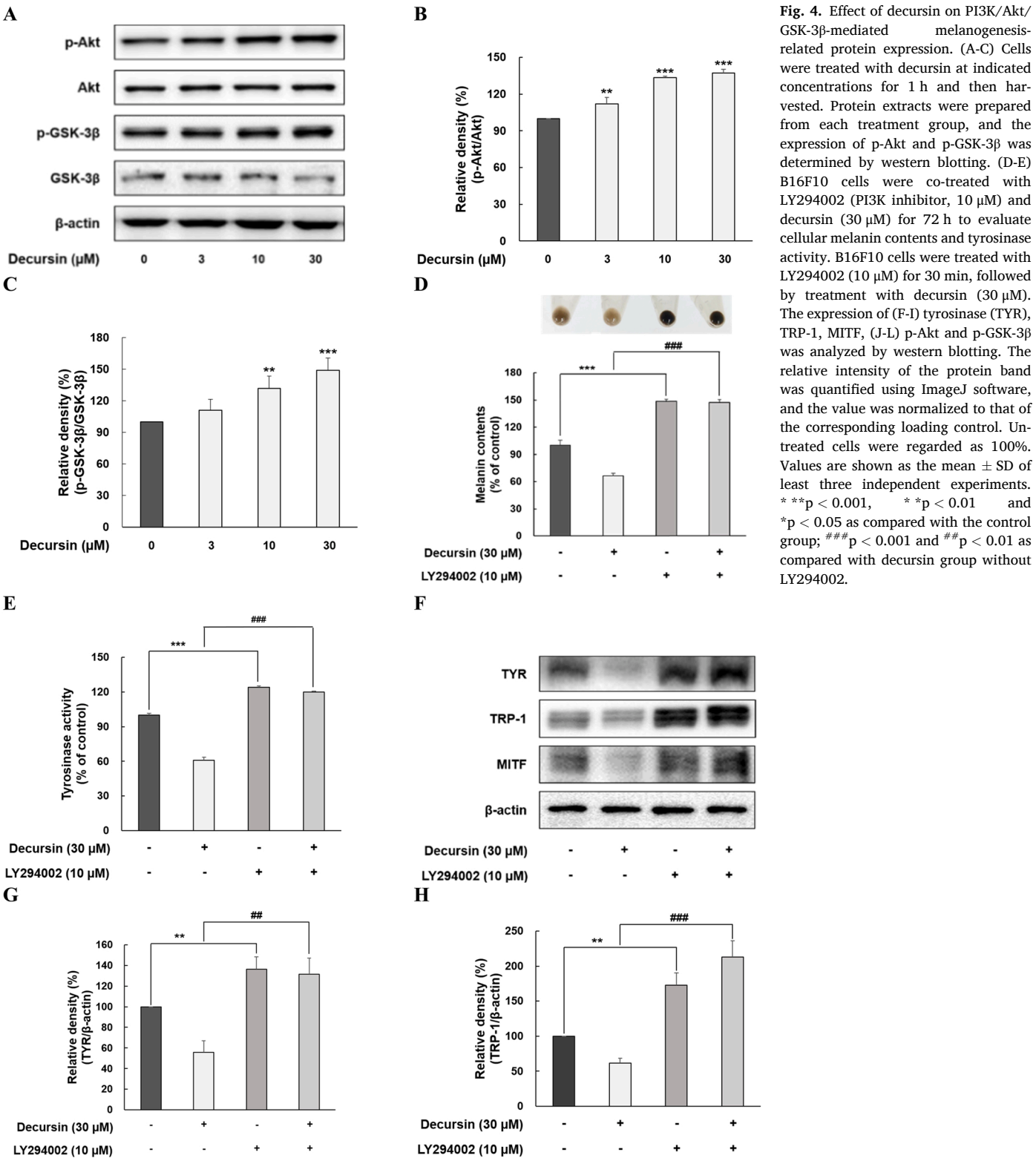

Fig. 4. Effect of decursin on PI3K/Akt/GSK-3β-mediated melanogenesis-related protein expression. (A-C) Cells were treated with decursin at indicated concentrations for 1 h and then harvested. Protein extracts were prepared from each treatment group, and the expression of p-Akt and p-GSK-3β was determined by western blotting. (D-E) B16F10 cells were co-treated with LY294002 (PI3K inhibitor, 10 μM) and decursin (30 μM) for 72 h to evaluate cellular melanin contents and tyrosinase activity. B16F10 cells were treated with LY294002 (10 μM) for 30 min, followed by treatment with decursin (30 μM). The expression of (F-I) tyrosinase (TYR), TRP-1, MITF, (J-L) p-Akt and p-GSK-3β was analyzed by western blotting. The relative intensity of the protein band was quantified using ImageJ software, and the value was normalized to that of the corresponding loading control. Untreated cells were regarded as 100%. Values are shown as the mean ± SD of least three independent experiments. $^{***}p < 0.001$, $^{**}p < 0.01$ and $^{*}p < 0.05$ as compared with the control group; $^{###}p < 0.001$ and $^{##}p < 0.01$ as compared with decursin group without LY294002.

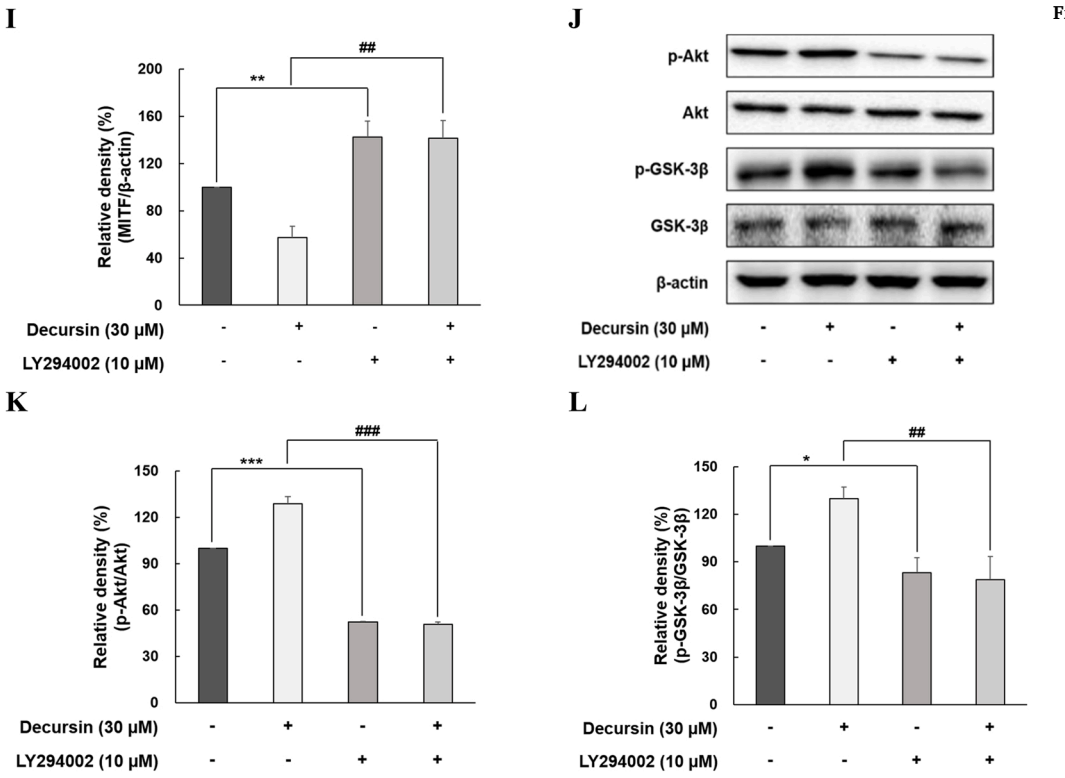

Fig. 4. (*continued*).

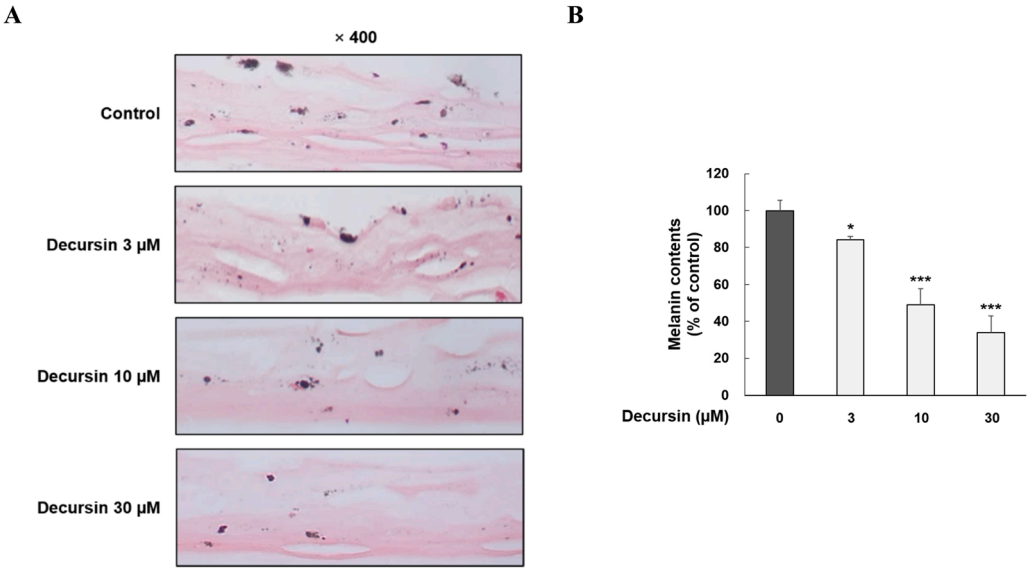

Fig. 5. Decursin suppresses melanin accumulation in an *ex vivo* human skin model. *Ex vivo* human skin tissues were pre-treated with decursin. After 15 days, skin tissues were harvested. (A) Representative images of Fontana-Masson-stained paraffin-embedded sections treated with control, 3 μM decursin, 10 μM decursin, and 30 μM decursin. (B) Quantification of melanin accumulation. * **$p < 0.001$ and *$p < 0.05$ as compared with the control group.

gastrointestinal (GI) tract. The results of the *in silico* toxicity risk assessment for decursin showed no sign of AMES and skin sensitization, suggesting its potential as a lead structure and justifying its anti-melanogenic activity in vivo.

4. Discussion

Although melanin synthesis is a beneficial mechanism that protects the skin from UV-induced DNA damage, excessive melanin deposition after exposure to UV radiation can lead to skin hyperpigmentation disorders [33]. Several approaches have been adopted to discover the components that could be employed to prevent skin hyperpigmentation disorders. The most commonly applied technique is an in vitro inhibitor screening assay that directly targets mushroom tyrosinase activity. However, the examination of active components identified using this method has often produced conflicting results because of intrinsic differences between the mushroom and mammalian tyrosinase used in the screening process and/or the effects of components that unexpectedly increased melanin synthesis depending on the cellular context [34]. As the most common hyperpigmentation disorders are associated with

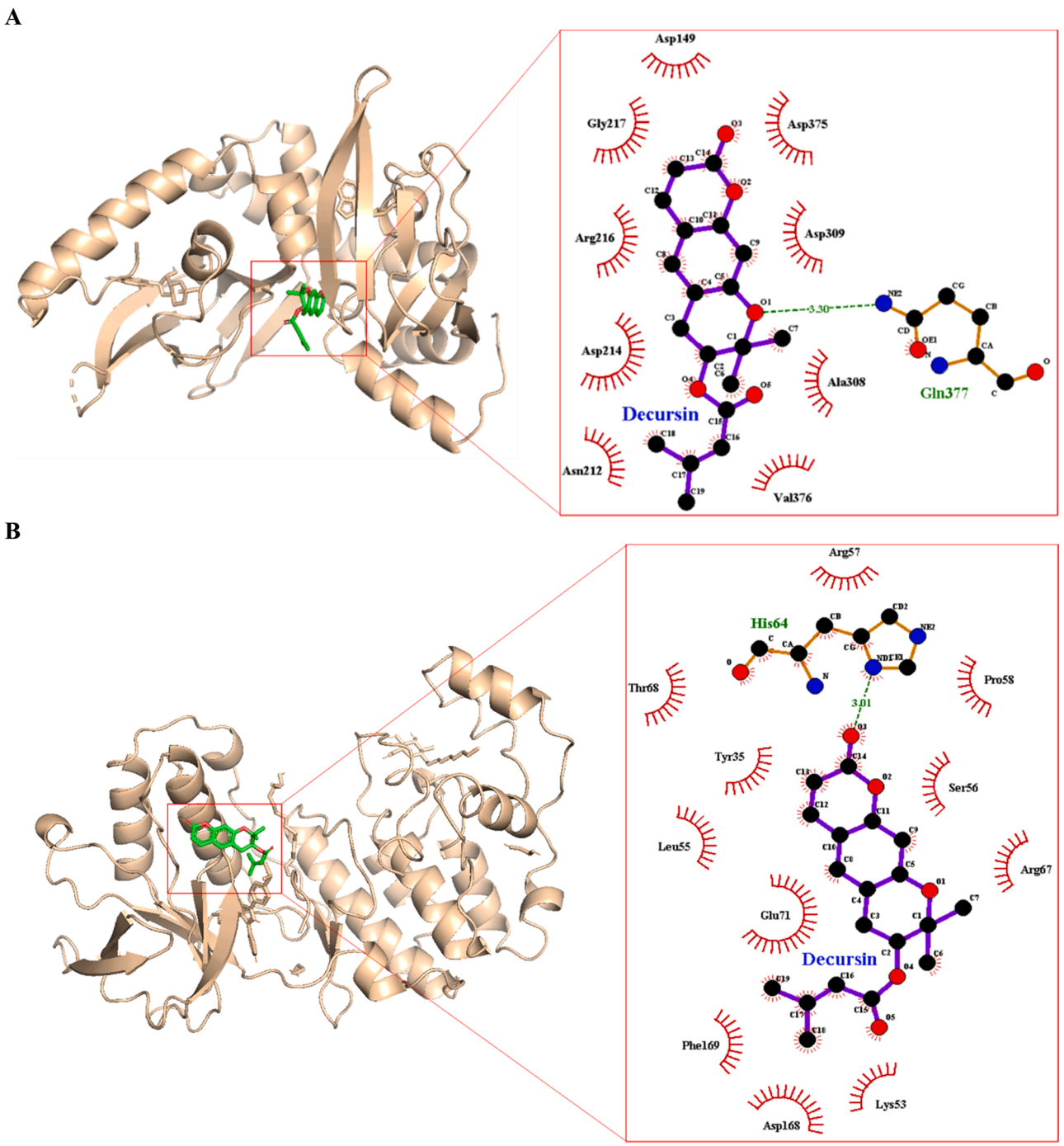

Fig. 6. Molecular docking interactions of decursin with (A) PKA, (B) p38, (C) ERK, and (D) PI3K; surface view and interaction map such as hydrogen (dotted line in green) and hydrophobic bonding (red dashed semicircle) between decursin and melanogenesis-related proteins. (For interpretation of the references to colour in this figure, the reader is referred to the web version of this article.)

MITF overexpression, recent studies have focused on developing better approaches via downregulation of MITF-mediated melanin accumulation [35,36].

To understand the mechanism of anti-melanogenic action of decursin in detail, the effect of the compound on the melanogenesis related enzymes was evaluated. Expression of tyrosinase and TRP-1 was decreased by decursin, which was consistent with the results of melanin synthesis. However, TRP-2 expression was not significantly altered by decursin, suggesting that our compound may not inhibit the action of MITF on the TRP-2 promoter. Further study is required to confirm the regulatory effect of decursin on MITF activity through gene expression at the promoter level. According to recent study, melanogenesis inhibitors such as resveratrol, hydroxyectoine, and lipoic acid-polyethylene glycol ester, have been reported to possess similar actions to decursin [37–39].

The expression of MITF is primarily modulated by cAMP/PKA-dependent activation, leading to the expression of melanogenic enzymes that eventually increase melanin production. In the present study, decursin inhibited CREB activation and consequently decreased MITF expression in B16F10 cells. Reduced MITF expression resulted in the downregulation of TYR and TRP-1 enzymes and suppression of melanin

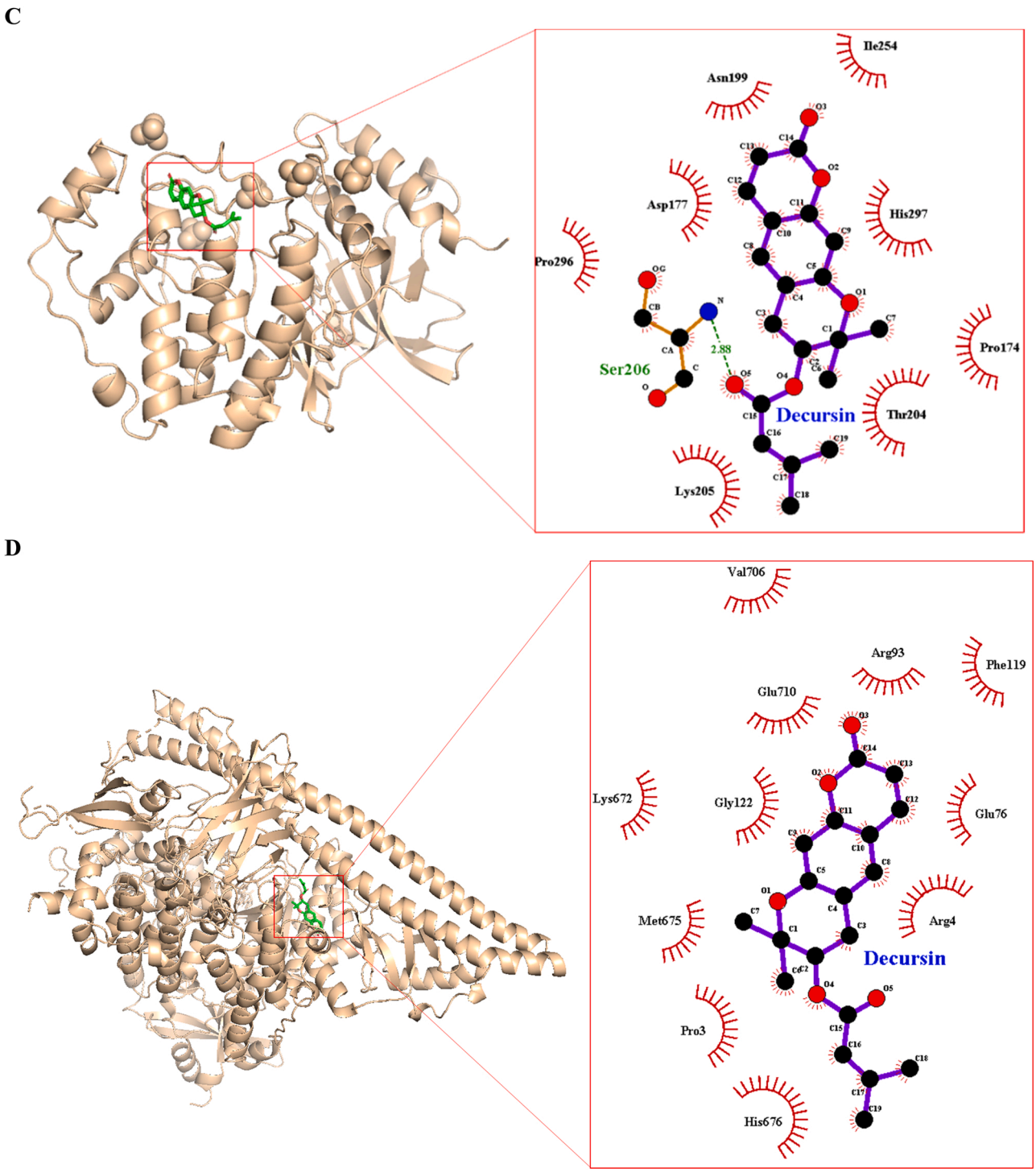

Fig. 6. (*continued*).

content. In addition, the inhibitory activity of decursin against tyrosinase partially contributed to reduced melanin production. Co-treatment with decursin and a PKA-specific inhibitor led to decreased melanin production than decursin treatment alone, demonstrating that MITF upregulation is mediated by the PKA/CREB signaling pathway. A recent study by Kim et al. (**2019**) demonstrated that CREB-dependent MITF expression inhibition by rottlerin successfully improved hyperpigmentation [36].

Previous studies have shown that hypopigmentation is controlled by MAPK-mediated MITF downregulation [11,12]. The present study revealed that the phosphorylation of p38 was significantly downregulated and ERK phosphorylation was considerably upregulated by decursin, leading to the suppression of MITF and tyrosinase family genes. However, this compound did not mediate a significant difference in the phosphorylation of JNK. Moreover, the involvement of p38 and ERK pathways was further confirmed by co-treatment of decursin with a p38 inhibitor (SB203580) or ERK inhibitor (PD98059), indicating that p38 and ERK were partially related to the hypopigmentation of decursin. A similar anti-melanogenic effect was also described where sulforaphane increased the level of phospho-ERK and reduced the abundance of phosphorylated p38 to inhibit melanogenesis [40].

PI3K/Akt/GSK-3β has been identified as another important signaling

Table 1
Molecular interaction of upstream regulators of MITF with decursin.

Targetprotein	Binding energy (kcal/mol)	No. of H-bonds	H-bonding residues	H-bond length (Å)	van Der Waals residues
PKA	− 7.8	1	Gln377	3.30	Asp149, Asn212, Asp214, Arg216, Gly217, Ala308, Asp309, Asp375, Val376
p38	− 8.0	1	His64	3.01	Tyr35, Lys53, Leu55, Ser56, Arg57, Pro58, Arg67, Thr68, Glu71, Asp168, Phe169
ERK	− 8.1	1	Ser206	2.88	Pro174, Asp177, Asn199, Thr204, Lys205, Ile254, Pro296, His297
PI3K	− 9.0	–	–	–	Pro3, Arg4, Glu76, Arg93, Phe119, Gly122, Lys672, Met675, His676, Val706, Glu710

Table 2
in Silico pharmacokinetic profiles of decursin using pkCSM.

Property	Decursin	Desired value
Human intestinal absorption (%)	97.3	< 30% (poorly absorbed)
Skin permeability (log K_p)	− 2.8	Low skin permeability > −2.5
AMES toxicity	No	No
Skin sensitization	No	No

cascade that regulates the transcriptional activity of MITF. Previous studies have shown that the activation of PI3K/Akt suppresses melanin accumulation in murine melanocytes and human melanoma Melan-A cells [41]. Inhibition of the AKT pathway by LY294002 increased melanin synthesis in B16F10 cells [42]. In this study, decursin augmented the phosphorylation of Akt and GSK-3β, leading to decreased expression of tyrosinase, TRP-1, and MITF. The PI3K-specific inhibitor LY294002 was used as a negative control to confirm the anti-melanogenic properties of decursin.

The 3D human skin models used in this study contain human melanocytes. The models were proven to show a similar morphology and physiology of human skin and the reliability of 3D human skin results has been proven through several studies [29–32,43]. Although cell-based systems have played an important role in discovering anti-melanogenic agent and its underlying molecular mechanism, not all results from these 2D cell culture systems are translatable to physiological in vivo system [29–32]. 2D cell culture systems lack the environmental factors (e.g. mechanical forces, spatial orientation, as well as physiological oxygen, nutrient and signaling gradients) associated within the 3D in vivo environment. Therefore, 3D human skin system serves as an important experimental model and as an animal alternative because it is more reliable than 2D skin cell cultures and less invasive than human skin biopsies. [43]. In the present study, decursin blocked melanogenesis in a dose-dependent manner in our *ex vivo* 3D human skin model. Interestingly, the anti-melanogenic efficacy of decursin at 10 μM concentration was two-fold higher in the reconstructed 3D human skin tissue than that of in cell culture system. Furthermore, depigmenting property of decursin at 3 μM was similar with that of arbutin as positive reference at 1 mM [44].

Another major finding of the present study was the identification of novel interactions of decursin with MITF upstream regulators. Decursin is closely bound to the active site of PKA (Asp309), which leads to the inhibition of PKA activation via binding to its regulatory subunit and interference in the binding of cAMP to PKA. The active site of p38 (Tyr35 and Lys53) was associated with hydrophobic interactions with decursin, proving that the compound inhibited the kinase by directly competing with ATP binding. In addition, the compound formed a hydrophobic interaction with Phe169, a pivotal residue that shuttles in different conformations in the active and inactive forms of p38 [45]. In contrast, decursin was observed to occupy a non-ATP catalytic site in ERK or PI3K, indicating that it is non-competitive with ATP.

Considering safety, decursin showed no sign of mutagenic response and skin sensitization during *in silico* toxicity risk assessment. Consistently, daily treatment with decursin (250 mg/kg, intraperitoneal administration for 4 weeks) exhibited no subacute toxic potential or adverse effects in Sprague-Dawley rats, confirming its safe nature [46]. Moreover, the compound showed good human intestinal absorption (97.3%) and skin permeability (−2.8 log *Kp*), which highlight its optimal potential and physiological benefits and/or biological efficacy in the prevention of hyperpigmentation disorders.

Pharmacokinetic studies in animal and human models suggested that the physiologically relevant dose of decursin was in the nanomolar range [47,48]. Li et al. showed the plasma concentration of decursin was mean peak concentration (C_{max}) of 43.7 ng/mL in rats after a single oral dose of decursin 50 mg/kg [47]. In addition, Zhang and coworkers (2015) investigated the pharmacokinetics of decursin in twenty healthy adults through extract of *A. gigas* Nakai [48]. A single administration of decursin at 119 mg established C_{max} of 5.3 nmol/L. The present *in silico* pharmacokinetic study revealed decursin to penetrate skin and absorb in human intestine when orally administered.

Although further in vivo research into the skin penetration of decursin is required, it is still meaningful that the present study offered a novel evidence which demonstrated that decursin exerted anti-melanogenic effects, pharmacokinetic properties, and safety through in vitro, *ex vivo*, and *in silico* approaches.

5. Conclusion

The present study demonstrates for the first time that decursin is a potent inhibitor of melanogenesis through suppression of MITF-mediated tyrosinase and TRP-1, but not TRP-2. The compound displayed multifunctional inhibitory activities on the melanogenesis pathway via PKA/CREB, p38/ERK MAPK, and PI3K/Akt/GSK-3β-mediated MITF degradation. Notably, the excellent anti-melanogenic effects of decursin on reconstructed human skin tissue, which is similar to the human epidermis, encourage its applicability in future clinical trials. *in Silico* analysis revealed that the compound not only had strong interactions with MITF upstream regulators but also exhibited optimal pharmacokinetic and safety profiles. This study provides a basis for elucidating a potential of decursin in preventing melanogenesis as well as a possibility for the use as a functional food, nutraceutical, nutricosmetics or food supplements.

CRediT authorship contribution statement

Hyungyeong Choi: Data curation, Validation, Writing – original draft. **Jeong-Hyun Yoon:** Data curation, Formal analysis. **Kumju Youn**: Data curation, Formal analysis, Writing – original draft. **Mira Jun**: Supervision, Data curation, Writing – review & editing. All authors have read and agreed to the final version of the manuscript.

Conflict of interest statement

The authors declare that they have no known competing financial interests or personal relationships that could have appeared to influence the work reported in this paper.

Acknowledgement

Funding: This research was funded by Dong-A University.

Appendix A. Supporting information

Supplementary data associated with this article can be found in the online version at doi:10.1016/j.biopha.2022.112651.

References

[1] A. Slominski, D.J. Tobin, S. Shibahara, J. Wortsman, Melanin pigmentation in mammalian skin and its hormonal regulation, Physiol. Rev. 84 (2004) 1155–1228, https://doi.org/10.1152/physrev.00044.2003.
[2] V. del Marmol, F. Beermann, Tyrosinase and related proteins in mammalian pigmentation, FEBS Lett. 381 (1996) 165–168, https://doi.org/10.1016/0014-5793(96)00109-3.
[3] N. Fuse, K. Yasumoto, H. Suzuki, K. Takahashi, S. Shibahara, Identification of a melanocyte-type promoter of the microphthalmia-associated transcription factor gene, Biochem. Biophys. Res. Commun. 219 (1996) 702–707, https://doi.org/10.1006/bbrc.1996.0298. ⟨https://doi⟩.
[4] E. Selzer, V. Wacheck, T. Lucas, E. Heere-Ress, M. Wu, K.N. Weilbaecher, W. Schlegel, P. Valent, F. Wrba, H. Pehamburger, D. Fisher, B. Jansen, The melanocyte-specific isoform of the microphthalmia transcription factor affects the phenotype of human melanoma, Cancer Res. 62 (2002) 2098–2103.
[5] M.L. Hartman, M. Czyz, MITF in melanoma: mechanisms behind its expression and activity, Cell. Mol. Life Sci. 72 (2015) 1249–1260, https://doi:10.1007/s00018-014-1791-0.
[6] D. Kumawat, V. Kumar, P. Sahay, G. Nongrem, P. Chandra, Bilateral asymmetrical partial heterochromia of iris and fundus in waardenburg syndrome type 2A with a novel MITF gene mutation, Indian J. Ophthalmol. 67 (2019) 1481–1483, https://doi:10.4103/ijo.ijo_931_17.
[7] X. Pang, X. Zheng, X. Kong, Y. Chai, Y. Wang, H. Qian, B. Yang, C. Wu, J. Chu, T. Yang, A Homozygous MITF mutation leads to familial waardenburg syndrome type 4, Am. J. Med. Genet. Part. A. 179 (2019) 243–248, https://doi:10.1002/ajmg.a.60693.
[8] Y. Ao, H.Y. Park, S. Olaizola-Horn, B.A. Gilchrest, Activation of cAMP-dependent protein kinase is required for optimal alpha-melanocyte-stimulating hormone-induced pigmentation, Exp. Cell Res. 244 (1998) 117–124, https://doi:10.1006/excr.1998.4086.
[9] J.C. Garcia-Borron, Z. Abdel-Malek, C. Jimenez-Cervantes, MC1R, the cAMP pathway, and the response to solar UV: extending the horizon beyond pigmentation, Pigment Cell Melanoma Res. 27 (2014) 699–720, https://doi.org/10.1111/pcmr.12257.
[10] M. Strnisková, M. Barancík, T. Ravingerová, Mitogen-activated protein kinases and their role in regulation of cellular processes, Gen. Physiol. Biophys. 21 (2002) 231–255.
[11] M. Wu, T.J. Hemesath, C.M. Takemoto, M.A. Horstmann, A.G. Wells, E.R. Price, D. Z. Fisher, D.E. Fisher, c-Kit triggers dual phosphorylations, which couple activation and degradation of the essential melanocyte factor Mi, Genes Dev. 14 (2000) 301–312.
[12] B. Saha, S.K. Singh, C. Sarkar, R. Bera, J. Ratha, D.J. Tobin, R. Bhadra, Activation of the Mitf promoter by lipid-stimulated activation of p38-stress signalling to CREB, Pigment Cell Res. 19 (2006) 595–605, https://doi:10.1111/j.1600-0749.2006.00348.x.
[13] K. Hughes, E. Nikolakaki, S.E. Plyte, N.F. Totty, J.R. Woodgett, Modulation of the glycogen synthase kinase-3 family by tyrosine phosphorylation, EMBO J. 12 (1993) 803–808, https://doi.org/10.1002/j.1460-2075.1993.tb05715.x.
[14] S. Frame, P. Cohen, GSK3 takes centre stage more than 20 years after its discovery, Biochem J. 359 (2001) 1–16, https://doi:10.1042/0264-6021:3590001.
[15] M. Khaled, L. Larribere, K. Bille, E. Aberdam, J.P. Ortonne, R. Ballotti, C. Bertolotto, Glycogen synthase kinase 3beta is activated by cAMP and plays an active role in the regulation of melanogenesis, J. Biol. Chem. 277 (2002) 33690–33697, https://doi:10.1074/jbc.M202939200.
[16] K.C. Ngeow, H.J. Friedrichsen, L. Li, Z. Zeng, S. Andrews, L. Volpon, H. Brunsdon, G. Berridge, S. Picaud, R. Fischer, R. Lisle, S. Knapp, P. Filippakopoulos, H. Knowles, E. Steingrímsson, K.L.B. Borden, E.E. Patton, C.R. Goding, BRAF/MAPK and GSK3 signaling converges to control MITF nuclear export, Proc. Natl. Acad. Sci. USA 115 (2018) E8668–E8677, https://doi:10.1073/pnas.1810498115.
[17] S.D. Sarker, L. Naharl, Natural medicine: the genus Angelica, Curr. Med. Chem. 11 (2004) 1479–1500, https://doi:10.2174/0929867043365189.
[18] S.S. Choi, K.J. Han, H.K. Lee, E.J. Han, H.W. Suh, Antinociceptive profiles of crude extract from roots of Angelica gigas NAKAI in various pain models, Biol. Pharm. Bull. 26 (2003) 1283–1288, https://doi:10.1248/bpb.26.1283.
[19] S. Lee, Y.S. Lee, S.H. Jung, K.H. Shin, B.K. Kim, S.S. Kang, Antitumor activities of decursinol angelate and decursin from Angelica gigas, Arch. Pharm. Res. 26 (2003) 727–730, https://doi:10.1007/BF02976682.
[20] S.Y. Kang, K.Y. Lee, M.J. Park, Y.C. Kim, G.J. Markelonis, T.H. Oh, Y.C. Kim, Decursin from Angelica gigas mitigates amnesia induced by scopolamine in mice, Neurobiol. Learn. Mem. 79 (2003) 11–18, https://doi:10.1016/s1074-7427(02)00007-2.
[21] S.Y. Kang, K.Y. Lee, S.H. Sung, Y.C. Kim, Four new neuroprotective dihydropyranocoumarins from Angelica gigas, J. Nat. Prod. 68 (2005) 56–59, https://doi:10.1021/np049705v.
[22] N. Lv, J.H. Koo, H.Y. Yoon, J. Yu, K.A. Kim, I.W. Choi, K.B. Kwon, K.S. Kwon, H. U. Kim, J.W. Park, B.H. Park, Effect of Angelica gigas extract on melanogenesis in B16 melanoma cells, Int. J. Mol. Med. 20 (2007) 763–767, https://doi.org/10.3892/ijmm.20.5.763.
[23] J. Zhang, L. Li, C. Jiang, C. Xing, S.H. Kim, J. Lü, Anti-cancer and other bioactivities of Korean Angelica gigas Nakai (AGN) and its major pyranocoumarin compounds, Anticancer Agents Med. Chem. 12 (2012) 1239–1254, https://doi:10.2174/187152012803833071.
[24] D.K. Jang, C.H. Pham, I.S. Lee, S.H. Jung, J.H. Jeong, H.S. Shin, H.M. Yoo, Anti-Melanogenesis activity of 6-O-Isobutyrylbritannilactone from Inula britannica on B16F10 Melanocytes and In Vivo Zebrafish Models, Molecules 25 (2020) 3887, https://doi:10.3390/molecules25173887.
[25] H.X. Li, J.U. Park, X.D. Su, K.T. Kim, J.S. Kang, Y.R. Kim, Y.H. Kim, S.Y. Yang, Identification of anti-melanogenesis constituents from Morus alba L. Leaves, Molecules 23 (2018) 2559, https://doi:10.3390/molecules23102559.
[26] R. Lee, H.J. Ko, K. Kim, Y. Sohn, S.Y. Min, J.A. Kim, D. Na, J.H. Yeon, Anti-melanogenic effects of extracellular vesicles derived from plant leaves and stems in mouse melanoma cells and human healthy skin, J. Extracell. Vesicles. 9 (2019), 1703480 https://doi:10.1080/20013078.2019.1703480.
[27] D.E. Pires, T.L. Blundell, D.B. Ascher, pkCSM: predicting small-molecule pharmacokinetic and toxicity properties using graph-based signatures, J. Med. Chem. 58 (2015) 4066–4072, doi: 10.1021/acs.jmedchem.5b00104.
[28] O. Trott, A.J. Olson, AutoDock Vina: improving the speed and accuracy of docking with a new scoring function, efficient optimization, and multithreading, J. Comput. Chem. 31 (2010) 455–461, https://doi:1;ll;0.1002/jcc.21334.
[29] M.W. Carlson, A. Alt-Holland, C. Egles, J.A. Garlick, Three-dimensional tissue models of normal and diseased skin, Curr. Protoc. Cell Biol. 19.9 (2008) https://doi:10.1002/0471143030.cb1909s41.
[30] M.J. Randall, A. Jüngel, M. Rimann, K. Wuertz-Kozak, Advances in the biofabrication of 3D skin in vitro: healthy and pathological models, Front. Bioeng. Biotechnol. 6 (2018) 154, doi:10.3389/fbioe.2018.00154.
[31] D.E. Kim, B.Y. Chang, S.O. Ham, Y.C. Kim, S.Y. Kim, Neobavaisoflavone inhibits melanogenesis through the regulation of Akt/GSK-3β and MEK/ERK pathways in B16F10 cells and a reconstructed human 3D skin model, Molecules 25 (2020) 2683, 10.3390/molecules25112683.
[32] L. Souci, C. Denesvre, 3D skin models in domestic animals, Vet. Res. 52 (2021) 21, 10.1186/s13567-020-00888-5.
[33] M. Brenner, V.J. Hearing, The protective role of melanin against UV damage in human skin, Photochem. Photobiol. 84 (2008) 539–549, https://doi:10.1111/j.1751-1097.2007.00226.x.
[34] T.Y. Song, C.H. Chen, N.C. Yang, C.S. Fu, Y.T. Chang, C.L. Chen, The correlation of in vitro mushroom tyrosinase activity with cellular tyrosinase activity and melanin formation in melanoma cells A2058, J. Food Drug Anal. 17 (2009) 156–162, https://doi.org/10.38212/2224-6614.2607.
[35] X. Yi, G. Zhao, H. Zhang, D. Guan, R. Meng, Y. Zhang, Q. Yang, H. Jia, K. Dou, C. Liu, F. Que, J.Q. Yin, MITF-siRNA formulation is a safe and effective therapy for human melasma, Mol. Ther. 19 (2011) 362–371, https://doi:10.1038/mt.2010.263.
[36] Y.H. Kim, D. Kim, A.R. Hong, J.H. Kim, H. Yoo, J. Kim, I. Kim, S.W. Kang, S. E. Chang, Y. Song, Therapeutic potential of rottlerin for skin hyperpigmentary disorders by inhibiting the transcriptional activity of CREB-regulated transcription coactivators, J. Invest. Dermatol. 139 (2019) 2359–2367, e2. https://doi:10.1016/j.jid.2019.05.012.
[37] S. Zhou, D. Riadh, K. Sakamoto, Grape extract promoted α-MSH-induced melanogenesis in B16F10 melanoma cells, which was inverse to resveratrol, Molecules 26 (2021) 5959, https://doi:10.3390/molecules26195959.
[38] Y.C. Chung, M.J. Kim, E.Y. Kang, Y.B. Kim, B.S. Kim, S.M. Park, C.G. Hyun, Anti-melanogenic effects of hydroxyectoine via MITF inhibition by JNK, p38, and AKT pathways in B16F10 melanoma cells, Nat. Prod. Commun. 14 (2019) 1–6, https://doi:10.1177/1934578×19858523.
[39] J.H. Kim, G.S. Sim, J.T. Bae, J.Y. Oh, G.S. Lee, D.H. Lee, B.C. Lee, H.B. Pyo, Synthesis and anti-melanogenic effects of lipoic acid-polyethylene glycol ester, J. Pharm. Pharm. 60 (2008) 863–870, https://doi:10.1211/jpp.60.7.0007.
[40] I. Shirasugi, M. Kamada, T. Matsui, Y. Sakakibara, M.C. Liu, M. Suiko, Sulforaphane inhibited melanin synthesis by regulating tyrosinase gene expression

in B16 mouse melanoma cells, Biosci. Biotechnol. Biochem. 74 (2010) 579–582, https://doi:10.1271/bbb.90778.
[41] M. Oka, H. Nagai, H. Ando, M. Fukunaga, M. Matsumura, K. Araki, W. Ogawa, T. Miki, M. Sakaue, K. Tsukamoto, H. Konishi, U. Kikkawa, M. Ichihashi, Regulation of melanogenesis through phosphatidylinositol 3-kinase-Akt pathway in human G361 melanoma cells, J. Invest. Dermatol. 115 (2000) 699–703, https://doi.org/10.1046/j.1523-1747.2000.00095.x.
[42] D.S. Kim, S.Y. Kim, J.H. Chung, K.H. Kim, H.C. Eun, K.C. Park, Delayed ERK activation by ceramide reduces melanin synthesis in human melanocytes, Cell. Signal. 14 (2002) 779–785, https://doi.org/10.1016/S0898-6568(02)00024-4.
[43] S. Eberlin, M.S.D. Silva, G. Facchini, G.H.D. Silva, A.L.T.A. Pinheiro, S. Eberlin, A. D.S. Pinheiro, The ex vivo skin model as an alternative tool for the efficacy and safety evaluation of topical products, Altern. Lab. Anim. 48 (2020) 10–22, https://doi:10.1177/0261192920914193.
[44] M. Lee, H. Park, S.W. Jeon, J. Bang, K.Y. Chung, D.W. Choi, E. Kim, K.M. Lim, Novel anti-melanogenic hexapeptoids, PAL-10 and PAL-12, Arch. Dermatol. Res. 307 (2015) 249–257, https://doi:10.1007/s00403-015-1555-1.
[45] V. Sahu, L. Nigam, V. Agnihotri, A. Gupta, S. Shekhar, N. Subbarao, S. Bhaskar, S. Dey, Diagnostic significance of p38 Isoforms (p38α, p38β, p38γ, p38δ) in head and neck squamous cell carcinoma: comparative serum level evaluation and design of novel peptide inhibitor targeting the same, Cancer Res. Treat. 51 (2019) 313–325, https://doi:10.4143/crt.2018.105.
[46] C. Jiang, J. Feng, J. Zhang, I. Han, S. Choung, Decursin safety from root of Angelica gigas in rats, J. Northeast Agric. Univ. 20 (2013) 46–51, https://doi.org/10.1016/S1006-8104(14)60046-5.
[47] L. Li, J. Zhang, C. Xing, S.H. Kim, J. Lü, Single oral dose pharmacokinetics of decursin, decursinol angelate, and decursinol in rats, Planta Med. 79 (2013) 275–280, https://doi:10.1055/s-0032-1328202.
[48] J. Zhang, L. Li, T.W. Hale, W. Chee, C. Xing, C. Jiang, J. Lü, Single oral dose pharmacokinetics of decursin and decursinol angelate in healthy adult men and women, PLoS One 10 (2015), e0114992 https://doi:10.1371/journal.pone.0114992.